

## Hybrid Separation Processes – Combination of Reactive Distillation with Membrane Separation

Carsten Buchaly, Peter Kreis, Andrzej Górak

*Department of Biochemical and Chemical Engineering, University of Dortmund, Emil-Figge-Str. 70,  
44227 Dortmund, Germany*

### Abstract

In this paper, the modelling, simulation and process analysis for a hybrid separation process, the combination of reactive distillation with membrane separation, is presented. The application is illustrated by the heterogeneously catalysed *n*-propyl propionate synthesis from 1-propanol and propionic acid. The membrane module is located in the distillate stream of the reactive distillation column in order to selectively remove the produced water without use of entrainers. Key aspects for the theoretical description of reactive distillation processes are discussed. For the stand-alone reactive separation process, the simulation results with a non-equilibrium model are in good agreement with experimental data obtained in a pilot scale column. Additionally, a comparison of the most common modelling depths, namely the non-equilibrium model with Maxwell-Stefan equations, the equilibrium model taking into account reaction kinetics and the equilibrium model assuming chemical equilibrium, is presented. Vapour permeation experiments using Sulzer Pervap<sup>TM</sup> 2201(D) have been performed in a pilot-scale membrane plant in order to determine the separation characteristics for the dewatering of the non-ideal binary 1-propanol-water mixture.

Keywords: hybrid process, reactive distillation, membrane separation, vapour permeation, experiments

### 1. Introduction

Over the years, the focus of the chemical and process industry has shifted towards the development and application of integrated processes combining the mechanism of reaction and separation in one single unit. This trend is motivated by benefits such as a reduction in equipment and plant size and improvement of process efficiency and safety, and hence a better process economy. Reactive distillation is an important example of a reactive separation process. Especially for equilibrium reactions like esterifications, ester hydrolysis and etherifications, the combination of reaction and separation within one zone of a reactive distillation column is a well-known alternative to conventional processes with sequential reaction and separation steps (Hiwale et al., 2004; Kaibel et al., 2005). In several cases, non-ideal aqueous-organic mixtures are formed which tend to form azeotropes. They can be overcome using

membrane separations like pervaporation and vapour permeation since they are very selective and not limited by vapour-liquid equilibrium (Rautenbach, 1997). Consequently, a hybrid process consisting of membrane-assisted reactive distillation contributes to sustainable process improvement due to arising synergy effects and allows for reduction of investment and operational costs.

A review of hybrid processes combining pervaporation with one or more other separation technologies can be found in (Lipnitski et al., 1999). The analysis of hybrid separation processes combining membrane separation with conventional distillation is described in (Kreis and Górak, 2006). An example for the investigation of a reactive hybrid process concept is the transesterification of methyl acetate and butanol to butyl acetate and methanol by the combination of reactive distillation and pervaporation, as examined by (Steinigeweg and Gmehling, 2004). The industrially operated hybrid process for the continuous production of fatty acid esters by reactive distillation and pervaporation is presented by (von Scala et al., 2005).

In this work, the heterogeneously catalysed esterification of propionic acid (ProAc) with 1-propanol (POH) to *n*-propyl propionate (ProPro) and water (H<sub>2</sub>O) is investigated:



The esterification reaction is reversible; the equilibrium constant is a weak function of temperature. As catalyst, the strongly acidic ion exchange resin Amberlyst 46<sup>TM</sup> from Rohm & Haas is used. Amberlyst 46<sup>TM</sup> has acidic active sites (sulfonic-acid groups) only at the surface of the styrene-co-divinylbenzene matrix (Lundquist, 1995). This catalyst shows thermal stability up to 120°C and is tailor-made for esterifications because the competing side product formations, e.g. etherification and dehydration of the alcohol, are suppressed (Blagov et al., 2006).

The chemical system shows complex thermodynamic phase behaviour with several binary and ternary azeotropes as well as miscibility gaps. Boiling points of the pure components and the azeotropic data of the system are shown in Table 1.

**Table 1:** Boiling points of pure components and azeotropic data at 1 atm (\*NIST, 2005, <sup>†</sup>Tlatlik, 2005, <sup>#</sup>Gmehling, 2004).

	T <sub>boil</sub> [°C]	Type	x <sub>POH</sub> [-]	x <sub>ProAc</sub> [-]	x <sub>ProPro</sub> [-]	x <sub>H<sub>2</sub>O</sub> [-]
POH*	97.2	-	1.0	-	-	-
H <sub>2</sub> O*	100.0	-	-	-	-	1.0
ProPro*	122.9	-	-	-	1.0	-
ProAc*	140.9	-	-	1.0	-	-
POH-ProPro-H <sub>2</sub> O <sup>†</sup>	86.2	heterogeneous	0.350	-	0.130	0.520
POH-H <sub>2</sub> O <sup>#</sup>	87.6	homogeneous	0.432	-	-	0.568
ProPro-H <sub>2</sub> O <sup>#</sup>	90.0	heterogeneous	-	-	0.350	0.650
ProAc-H <sub>2</sub> O <sup>#</sup>	99.9	homogeneous	-	0.050	-	0.950

Due to two binary homogeneous azeotropes (1-propanol–water, propionic acid–water), one binary heterogeneous (*n*-propyl propionate–water) as well as one ternary heterogeneous (*n*-propyl propionate–1-propanol–water) temperature minimum

azeotrope, a conventional process requires a complex separation train downstream of the reactor.

## 2. Process description

One possible process alternative for *n*-propyl propionate synthesis in one apparatus is the removal of the desired product (ProPro) at the bottom of the reactive distillation column while at the top, an almost azeotropic aqueous-organic mixture (POH/H<sub>2</sub>O) is obtained. A hydrophilic membrane unit is located in the distillate stream to remove water out of the process. The water depleted retentate is recycled back to the column. The coupling of the reactive distillation column with a membrane module results in a hybrid process (Figure 1).

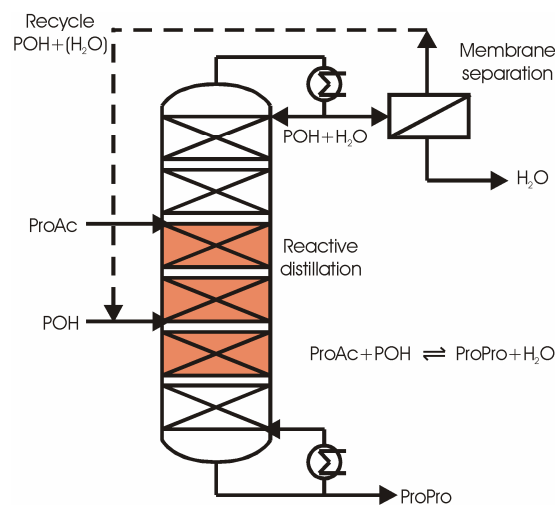


**Figure 1:** Reactive distillation column with a membrane separation located in the distillate stream.

## 3. Reactive distillation – modelling

Numerous papers about the modelling of reactive distillation processes can be found in the literature; comprehensive reviews about this topic are written by (Taylor and Krishna, 2000; Noeres et al., 2003; Kenig und Górak, 2007; Richter et al., 2006). They identify the key aspects for the proper description of reactive distillation processes being as follows:

- the description of thermodynamic and physical properties of the multicomponent system,
- the use of accurate reaction kinetics,
- the modelling of mass and heat transfer between liquid and vapour phase,
- the hydraulic characteristics of the column internals in terms of correlations for hold-up and pressure drop and
- the validation of the proposed process model with reliable experimental data.

These aspects are analysed in this paper.

### 3.1. Thermodynamic and physical properties

For the calculation of thermodynamic and physical properties, the software package Aspen Properties<sup>TM</sup> (www.aspentech.com) is used. The UNIQUAC model for the calculation of the activity coefficients in the liquid phase is applied to take into account the liquid phase non-idealities. The binary interaction parameters  $a_{ij}$  and  $b_{ij}$  used are summarised in Table 2.

**Table 2:** UNIQUAC binary interaction parameters  $a_{ij}$  and  $b_{ij}$

Component 1	Component 2	i	j	$a_{ij}$	$b_{ij}$ (K)
1-propanol	Propionic acid	1	2	0.0	-145.7
		2	1	0.0	183.9
<i>n</i> -propyl propionate	Water	1	2	6.743	-3266
		2	1	2.193	-887.6
1-propanol	Water	1	2	1.839	-669.0
		2	1	-2.409	620.8
Propionic acid	Water	1	2	0.0	73.80
		2	1	0.0	-244.8
<i>n</i> -propyl propionate	Propionic acid	1	2	0.0	-229.4
		2	1	0.0	119.9
1-propanol	<i>n</i> -propyl propionate	1	2	0.0	-1.924
		2	1	0.0	-87.25

The Hayden-O'Connell equation of state (Hayden and O'Connell, 1975) is chosen to take into account the non-idealities in the vapour phase, e.g. the dimerisation of the carbonic acid.

### 3.2. Reaction kinetics

The use of accurate data for the reaction kinetics is crucial for a predictive column design. For the modelling of the heterogeneously catalysed synthesis of *n*-propyl propionate, a pseudo-homogeneous approach is applied:

$$r_i = m_{cat,dry} \cdot V_i \cdot c_{act} \cdot \left( k_1(T) \cdot a_{PrOAc} \cdot a_{POH} - \frac{k_1(T)}{K_{eq}(T)} \cdot a_{PrOPro} \cdot a_{H_2O} \right), \quad i = 1, \dots, n_c. \quad (2)$$

The temperature dependency on the activity-based equilibrium constant  $K_{eq}$  as well as the rate constant of the forward reaction  $k_1$  are taken into account via the Arrhenius approach. Both parameters have been measured in the expected operating range of the reactive distillation column (Duarte et al., 2006).

$$k_1(T) = 7.381 \cdot 10^7 \cdot \exp \left\{ \frac{-5.963 \cdot 10^4}{R_m \cdot T} \right\} \quad (3)$$

$$K_{eq}(T) = 6.263 \cdot \exp \left\{ \frac{4.519 \cdot 10^3}{R_m \cdot T} \right\} \quad (4)$$

### 3.3. Reactive distillation model

In this work, a non-equilibrium stage model (NEQ model) is applied, which considers both the multicomponent mass transfer as well as heat transfer rates (Klöker et al., 2005; Górak and Hoffmann, 1999; Schneider et al., 1999). The influence of the hydrodynamic is taken into account by packing-specific correlations for mass-transfer coefficients in the vapour and liquid phase, interfacial area, liquid hold-up and pressure drop. The catalytic section of the reactive distillation column is equipped with the reactive structured packing Katapak-SP (type 11, Sulzer Chemtech); the structured packing Sulzer BX is used inside of the enrichment and stripping section. The required correlations are taken from the literature and are summarised for both packing types in Table 3.

**Table 3:** Correlations for both used packing types ( $\varnothing_{\text{column}} = 50 \text{ mm}$ ).

	Katapak SP-11	Sulzer BX
Gas-phase mass-transfer coefficient, $k_G$	Brunazzi 2006 (Brunazzi, 2006)	Bravo 1985 (Bravo et al., 1985)
Liquid-phase mass-transfer coefficient, $k_L$	Brunazzi 2006 (Brunazzi, 2006)	Bravo 1985 (Bravo et al., 1985)
Effective interfacial area, $a_{\text{eff}}$	Brunazzi 2006 (Brunazzi and Viva, 2006)	Rocha 1993 (Rocha et al., 1993)
Liquid hold-up, $h_L$	Brunazzi 2006 (Brunazzi and Viva, 2006)	Rocha 1993 (Rocha et al., 1993)
Pressure drop, $\Delta p$	Brunazzi 2006 (Brunazzi and Viva, 2006)	Rocha 1993 (Rocha et al., 1993)

All model equations are implemented into the simulation environment Aspen Custom Modeler<sup>TM</sup>. The peripherals, e.g. reboiler and condenser are assumed to be ideal. Furthermore, an extended equilibrium stage model (EQ model) is available in the simulation environment. This enables an analysis regarding the proper choice of the modelling depth which is required for a reliable process simulation.

## 4. Reactive distillation – experiments

For model validation purposes, a series of reactive distillation experiments have been carried out in a glass column with an inner diameter of 50 mm at atmospheric pressure. The set-up has a separation section below (0.5 m) and above (2.4 m) the reactive section (2.6 m). A total packing height of 5.5 m is realised. The characteristics of the pilot plant are summarised in Table 4.

The mass of dry catalyst per meter of catalytic packing has been determined experimentally to  $m_{\text{cat,dry}} = 0.205 \text{ kg}_{\text{cat,dry}}/\text{m}_{\text{packing}}$ , whereas the activity of the catalyst has been measured to  $c_{\text{act}} = 0.78 \text{ eq}/\text{kg}_{\text{cat,dry}}$  after the reactive distillation experiments

have been successfully performed. The titration procedure was in accordance with DIN standard 54403 (DIN, 2000).

A comparison between representative experimental results and model prediction is given in Figure 2, in which the liquid-phase molar fraction as well as the vapour temperature profiles is shown along the packing height.

**Table 4:** Reactive distillation - pilot plant characteristics

Pilot plant column	
Column diameter	50 mm
Rectifying section	2.4 m (Sulzer BX)
Reactive section	2.6 m (Katapak-SP 11)
Stripping section	0.5 m (Sulzer BX)
Pressure	Atmospheric

It should be emphasised that no side product (di-*n*-propyl ether, DPE) was detected by gas chromatography and no parameter fitting is carried out. Due to an excess of 1-propanol and a sufficient amount of catalyst, the propionic acid is nearly completely converted in the reactive section ( $X_{ProAc} = 94.8\%$ ). *N*-propyl propionate leaves the column as a bottom product beside non-converted propionic acid. In this experiment, the molar fraction of  $x_{ProPro} = 0.85$  is achieved in the bottom stream. At the top of the column, an almost binary mixture consisting of 1-propanol and water near to azeotropic composition with a small amount of *n*-propyl propionate is obtained. The simulation results are displayed with continuous lines. Both the composition profiles and the temperature profile are predicted with high accuracy. Further details about the experimental work will be published soon.

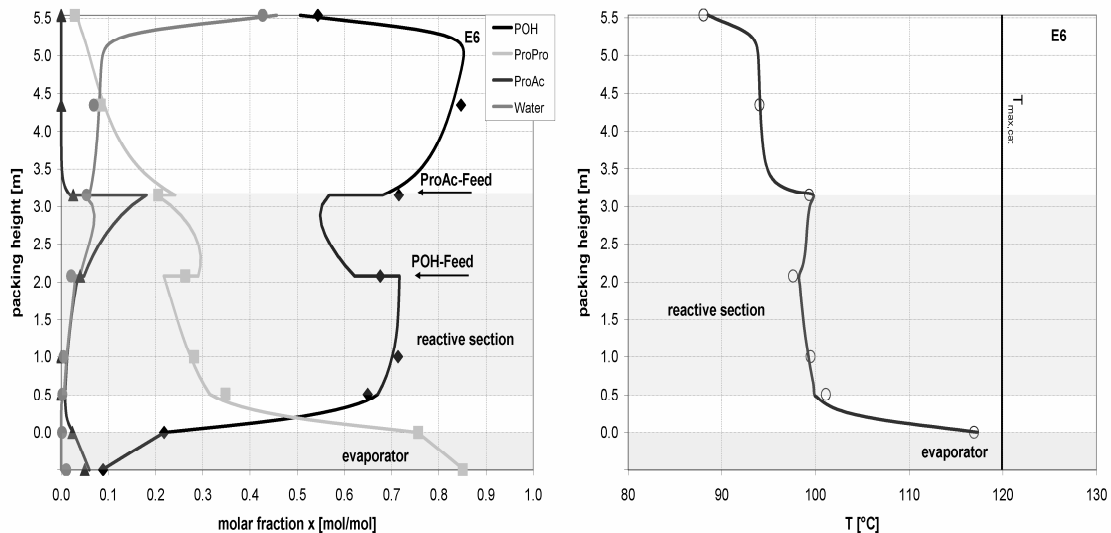


**Figure 2:** Liquid phase molar fraction (left) and temperature profile of the vapour phase (right) for experiment E6 (feed stream: 1.98 kg/h, RR: 2.49, D/Fmass: 0.424, molar feed ratio POH/ProAc: 2.068). The solid lines represent the simulation results, the symbols the experimental values (Buchaly et al., 2006).

## 5. Influence of modelling depth

The choice of an appropriate modelling depth, e.g. the use of the EQ or NEQ model for reactive distillation is not a trivial decision and has to be verified for each specific separation task. The EQ model requires knowledge of the separation efficiency in terms of a plate efficiency or HETP value. It is a lumped parameter which is constant for all components over the entire concentration range. On the other hand, the use of a NEQ model requires several model parameters, like mass-transfer coefficients, specific interfacial area as well as several additional physical properties, e.g. diffusion coefficients and surface tension. The most common modelling depths,

- the non-equilibrium model,
- the equilibrium model taking into account the reaction kinetics and
- the equilibrium model assuming chemical equilibrium,

have been applied in this paper. Since the desired product, *n*-propyl propionate, is removed via the bottom stream of the reactive distillation column, the impacts of the different modelling depths are investigated by a varying of the catalyst volume fraction,  $\psi_{cat}$ , and its influence on the acid conversion and therefore on the composition of the bottom stream (Figure 3). For both EQ model calculations a constant HETP value of 0.146 is used for the Sulzer BX packing, which has been extrapolated from (Sulpak, 2001), while a constant HETP value of 0.5 is applied for the structured catalytic packing Katapak-SP 11 (Steinigeweg and Gmehling, 2004). In this investigation the separation efficiency is considered as independent from the F-factor (F-factors between 0.4 and 0.5 Pa<sup>0.5</sup>).

For the EQ model assuming chemical equilibrium the composition of the bottom stream is independent of  $\psi_{cat}$ , showing a product purity of  $x_{ProPro,bottom} = 86.5\%$ , while  $x_{POH,bottom} = 13.3\%$  and  $x_{ProAc,bottom} = 0.2\%$ .

The validated reference NEQ model shows a strong influence of the catalyst volume fraction on the composition of the bottom stream up to  $\psi_{cat} = 80\%$ . With an increase in the amount of catalyst, which leads to a higher conversion of the propionic acid, an increase in the product purity can be achieved. Since an excess of alcohol is used, the 1-propanol composition is almost independent in the investigated range of catalyst volume fraction. The EQ model with reaction kinetics shows qualitatively similar results. Since the reaction is far from chemical equilibrium, the necessity of applying reaction kinetics for a proper description of the *n*-propyl propionate synthesis, which is a kinetically controlled reaction, is confirmed. To achieve the equilibrium conversion, an unrealistic catalyst volume fraction of  $\psi_{cat} = 160\%$  is required for the EQ model with reaction kinetics.

It can be shown that especially for the actual catalyst amount of the pilot-scale column (DN 50,  $\psi_{cat} = 23\% \cong m_{cat,dry} = 0.205 \text{ kg/m}$ ), in which the experimental validation has been performed, a lower product purity ( $x_{ProPro,bottom} = 77\%$ ) is predicted by the EQ model in comparison to the NEQ model ( $x_{ProPro,bottom} = 80\%$ ). In this range, the strongest influence of  $\psi_{cat}$  on conversion and thus the product purity is observed.

Our extensive simulation studies allow for the following conclusions:

- The EQ model assuming chemical equilibrium is not sufficient for the correct description of the n-propyl propionate synthesis in a reactive distillation column in laboratory and pilot-scale.
- The use of accurate reaction kinetic data is crucial, especially in the evaluation of experimental investigations performed in laboratory and pilot-scale columns. This high sensitivity at low catalyst volume fractions was also emphasised by Schmitt (Schmitt, 2005). For industrial-scale columns, where the catalyst volume fraction is remarkably higher ( $\psi_{cat} = 45\text{--}55\%$ ), the sensitivity towards the reaction kinetic data is lower.
- The reference NEQ model shows about 3 % higher product purity in comparison to the EQ model using reaction kinetics.

A detailed analysis and comparison of the EQ model with reaction kinetics and the NEQ model is in progress.

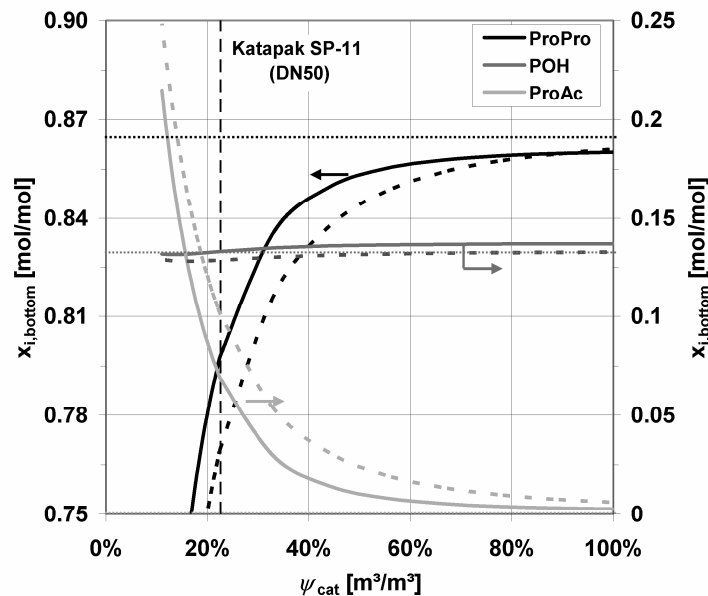


**Figure 3:** Influence of the modelling depth on the composition of the bottom stream of the reactive distillation column. Non-equilibrium model (solid lines), equilibrium model using reaction kinetics (dashed lines) and equilibrium model assuming chemical equilibrium (dotted lines).

## 6. Vapour permeation

In vapour permeation, volatile components are separated by a non-porous membrane due to different sorption and diffusion properties. Consequently, the separation is very selective and not limited by the vapour-liquid equilibrium. The driving force is generated by lowering the partial pressure of the favourable permeating component on the permeate side by applying a vacuum. In vapour permeation, the feed is supplied as vapour, whereas in pervaporation, the feed stream enters the membrane module as liquid. For the coupling of a membrane separation unit with a reactive distillation column, the membrane is operated in vapour permeation mode to avoid polarisation effects in the boundary layer adjacent to the membrane surface at low feed streams.



### 6.1. Experimental setup

Vapour permeation experiments are carried out in a pilot-scale plant equipped with a plate and frame membrane module from Sulzer Chemtech and an effective membrane area of 0.5 m<sup>2</sup> to determine the separation characteristics of the used hydrophilic membrane. A sketch of the plant is shown in Figure 4. The liquid feed mixture is heated-up to boiling conditions in the feed vessel B1. The degree of superheating of the arising vapour is adjusted in the heat exchanger W1. Temperature measurements are performed inside the feed vessel, before and after the heat exchanger as well as at the outlet of the retentate and permeate stream. The permeate pressure is maintained by a vacuum pump P1. The retentate is condensed in condenser W2, collected in vessel B2 and recycled back to the feed vessel with gear pump P2. A chilling unit consisting of two serial heat exchangers W3 and W4 is applied for condensation of permeate under vacuum, whereas cooling brine is used here. The condensed permeate is collected in vessel B3 and recirculated into the feed vessel by the membrane pump P3, which enables a continuous measurement of the permeate flux. All pipes and the membrane module are insulated and heat traced in order to prevent heat losses and condensation. The plant is equipped with a process control system and can therefore be operated automatically to ensure steady-state conditions.

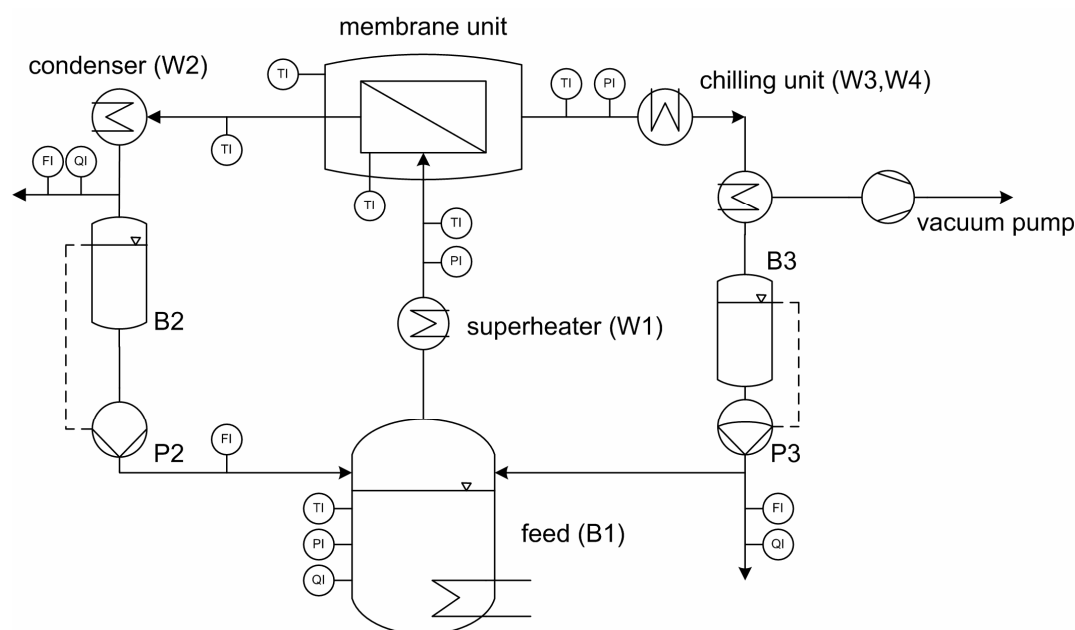


**Figure 4:** Pilot-scale experimental setup for vapour permeation.

In this work, the polymeric membrane Pervap<sup>TM</sup> 2201(D) from Sulzer Chemtech is applied. It consists of an active polyvinylalcohol (PVA) layer and a polyacrylnitrile (PAN) support layer to ensure its mechanical strength (van Baelen et al., 2004).

### 6.2. Analytics

Feed, retentate and permeate samples are analysed with the aid of gas chromatography to determine the mass fraction of the organic component. The gas chromatography device has been supplied by Shimadzu (GC14A with FID; He as

carrier gas with 30 ml/s; CS-FS-FFAP column (25 m · 0.32 mm) and a film thickness of 0.5  $\mu\text{m}$ ; split-ratio 1:100; temperature program: 343 K for 3.5 min, heat rate of 30 K min<sup>-1</sup> to 423 K hold for 3 min). For the determination of water content, Karl-Fischer titration is applied (Mettler Toledo DL 31; reagents: methanol, Hydranal Composite 5).

### 6.3. Experimental investigation

Experiments with a binary 1-propanol/water mixture are performed in order to investigate the separation behaviour of Sulzer Pervap<sup>TM</sup> 2201(D) with a membrane area of  $A_{memb} = 0.5 \text{ m}^2$  to deplete the obtained distillate stream of the column. The experimental data and operating conditions are summarised in Table 5.

**Table 5:** Experimental data for the operating conditions of the vapour permeation experiments

$\dot{m}_{ret}$ [kg/h]	$J_{total}$ [kg/m <sup>2</sup> h]	$w_{H2O,feed}$ [kg/kg]	$w_{H2O,ret}$ [kg/kg]	$w_{H2O,perm}$ [kg/kg]	$T_{feed}$ [°C]	$\Delta T_{sup}$ [°C]	$p_{feed}$ [bar]	$p_{perm}$ [mbar]
3.92	0.65	0.136	0.072	0.912	91.6	0.0	1.077	98
3.96	0.66	0.132	0.067	0.921	91.7	0.0	1.075	71
3.90	0.69	0.134	0.064	0.919	91.7	0.0	1.077	71
3.82	0.69	0.131	0.059	0.932	91.8	0.0	1.080	31
2.76	1.55	0.282	0.092	0.957	92.0	2.8	1.095	71
2.73	1.55	0.281	0.090	0.958	92.0	2.8	1.096	71
3.22	1.46	0.243	0.081	0.956	91.6	2.2	1.104	31
1.99	1.50	0.291	0.053	0.920	101.9	2.4	1.603	31
1.96	1.48	0.290	0.053	0.920	102.3	2.8	1.600	31
1.89	1.44	0.295	0.056	0.919	102.4	3.0	1.590	71
1.12	0.86	0.298	0.058	0.922	98.4	10.3	1.032	31
1.16	0.89	0.299	0.059	0.921	97.5	9.4	1.033	32
1.13	0.85	0.296	0.060	0.925	98.7	10.6	1.033	32

It can be seen that the separation characteristics show a strong dependency on the feed concentration. Since the active layer of the membrane consists of PVA, swelling of the polymeric membrane occurs with higher water concentrations in the feed. Water molecules form hydrogen bonds with the hydroxyl groups inside the polymeric matrix, causing the swelling phenomena (Stange, 2001).

### 6.4. Modelling of vapour permeation

For the modelling and simulation of the vapour permeation a detailed and flexible simulation model based on the “solution-diffusion theory” is applied (Rautenbach, 1997). Various modelling approaches for the calculation of the transmembrane flux are implemented (Table 6). The model considers the influence of fluid dynamics, porous support layer and non-ideal effects like concentration and temperature polarisation on the process performance. For further details, refer to (Kreis and Górak, 2005). In this work, an empirical correlation based on two parameters for each

component in accordance with Table 6 is applied as a transport equation to calculate the transmembrane flux as a function of the water concentration in the membrane feed stream.

**Table 6:** Implemented modelling approaches for the calculation of the transmembrane flux

Mass transport model	Permeance $Q_i$	
Short-cut model (SC)	$Q_i^0$	Constant
Empirical correlation (C)	$Q_i^0 \cdot w_{i,Feed}^A$	$\Delta DF$ : partial pressure
Arrhenius approach (AH)	$Q_i^0 \cdot \exp\left(-\frac{E_i}{R} \cdot \left(\frac{1}{T^0} - \frac{1}{T}\right)\right)$	T-dependent
Meyer-Blumenroth (MB)	$\frac{\tilde{D}_i(T)}{\tilde{\gamma}_i}$	$\Delta DF$ : activities
Hoemmerich (HO)	$A_i^* \cdot \frac{b_i(T) \cdot a_i^F}{1 + b_i(T) \cdot a_i^F} \cdot \frac{1}{\tilde{a}_i}$	$\Delta DF$ : activities
Sorption-diffusion (SD)	$\frac{\tilde{c}_i(T) \cdot \tilde{D}_i(T)}{\tilde{f}_i(T)} \cdot \frac{1}{\delta_M}$	$\Delta DF$ : activities

The empirical model does not take into account the temperature dependency. All required parameters are determined by the minimum least square regression method and are listed in Table 7. The comparison of simulated and experimental permeate fluxes is illustrated in the parity plot in Figure 5 and indicates good agreement over the investigated concentration range.

**Table 7:** Determined parameters for the empirical correlation used.

Component	$Q_i^0$	$A$
Water	897.8	0.74
1-propanol	1.22	0.0

## 7. Process analysis of membrane assisted reactive distillation

The analysis of the hybrid separation process shows high complexity in comparison to the stand-alone unit-operations, reactive distillation and vapour permeation. Thus, the presented validated process models for both units are linked together to enable a theoretical analysis of the hybrid separation process. Both the influence of decisive operational parameters, reboiler heat duty and reflux ratio, on the process performance in terms of product purity and acid conversion and the effect of a variation of the recycle purity are analysed.

### 7.1. Influence of reflux ratio and reboiler heat duty

The influence of the reboiler heat duty on product purity,  $x_{ProPro, bottom}$ , and on conversion of propionic acid,  $X_{ProAc}$ , for different reflux ratios is shown in Figure 6. At the endpoint of the curves, flooding of the catalytic packing internals occurs.

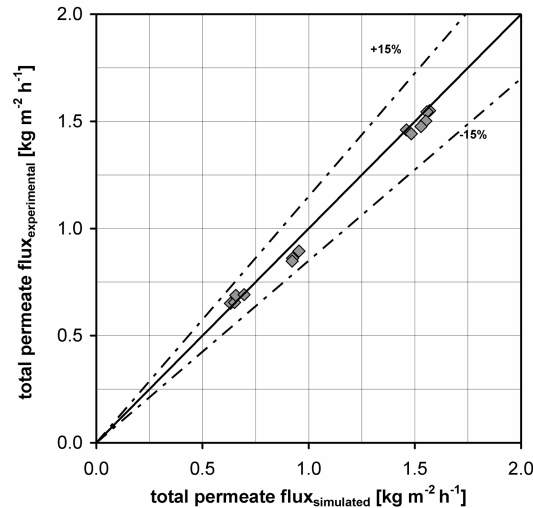


**Figure 5:** Simulated versus experimentally measured permeate fluxes.

The reflux ratio and reboiler heat duty have been varied from 1.5-3.0 and 900-1500 W, respectively. On one hand, the required reboiler heat duty increases with higher reflux ratio to achieve the required product purity (Figure 6, left). On the other hand, it can be seen that the conversion of the propionic acid increases with reduced reboiler heat duty (Figure 6, right).

### 7.2. Variation of reflux purity

The degree of dewatering is mainly defined by the realised membrane area in the distillate stream. While permeate, which consists mainly of water, is removed out of

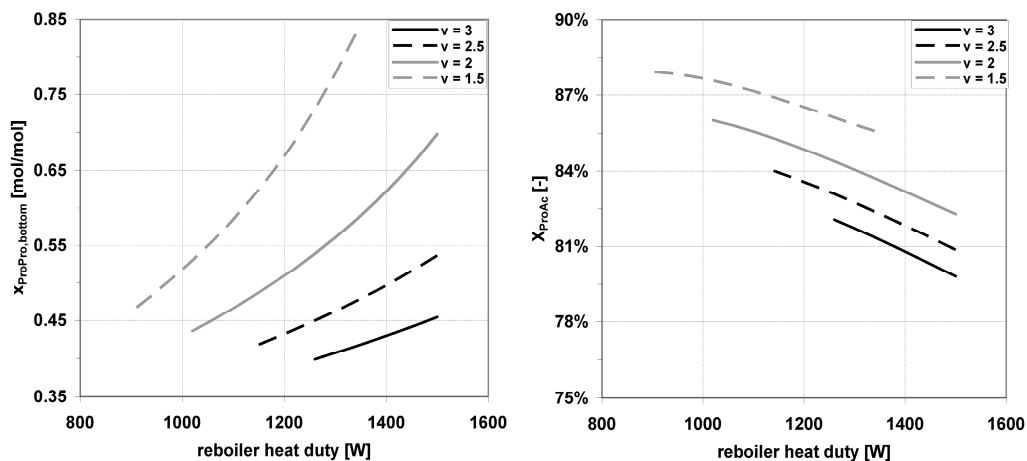


**Figure 6:** Influence of reboiler heat duty and reflux ratio,  $v$ , on product purity,  $x_{ProPro, bottom}$  (left) and propionic acid conversion,  $X_{ProAc}$  (right).

the process, the remaining water in the retentate stream of the membrane module is recycled back with non-converted 1-propanol. This leads to an enrichment of water in the reactive distillation column, causing an increase of both the internal flows as well as the required reboiler heat duty. Figure 7 illustrates the influence of the reflux purity, namely the mass fraction of water in the recycle stream,  $w_{H2O,recycle}$ , on both the required membrane area as well as reboiler heat duty. In this simulation study, the distillate stream as well as the reflux ratio is kept constant.

The membrane area is decreasing exponentially with an increase of  $w_{H2O,recycle}$ . Comparatively large membrane areas are required for an almost complete dewatering ( $w_{H2O,recycle} = 0.5\%$ ;  $A_{memb} = 2.0 \text{ m}^2$ ). This is due to the fact that the driving force for the water permeation diminishes at low water mass fractions. To achieve moderate membrane areas, lower reflux purities ( $w_{H2O,recycle} > 2.5\%$ ) are necessary. In contrast, the reboiler heat duty is increasing linear with increasing mass fraction of water in the recycle stream.

This leads to an optimisation problem which can only be solved taking into account the operating and investment costs of both unit operations.

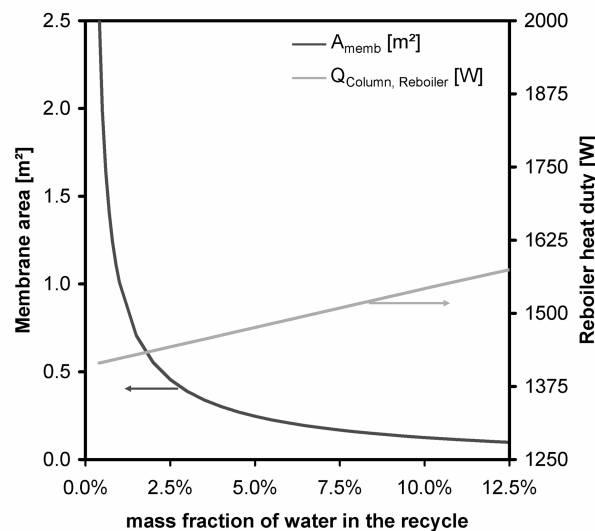


Figure 7: Influence of the mass fraction of water in the recycle on required membrane area and reboiler heat duty.

## 8. Conclusion

The theoretical and experimental investigation shows that the heterogeneously catalysed synthesis of n-propyl propionate via a hybrid process consisting of reactive distillation and vapour permeation is feasible.

For the simulation of the reactive distillation column, a NEQ model has been applied. Based on a series of reactive distillation experiments, a successful model validation has been performed. The most common modelling depths for the description of the reactive distillation process, namely the NEQ model, the EQ model taking into account reaction kinetics and the EQ model assuming chemical equilibrium, have been compared. One major result of this study is that the EQ model assuming chemical equilibrium is not sufficient for a proper description of the n-propyl propionate synthesis in a reactive distillation column at laboratory and pilot-scale. The NEQ model and the EQ model with reaction kinetics exhibit qualitatively similar

results over a broad range of catalyst volume fractions. For a detailed comparison of the NEQ model and the EQ model with reaction kinetics, further studies are necessary. The simulation study shows that accurate reaction kinetic data is crucial for the investigation of the reactive distillation process in laboratory and pilot-scale columns. Industrial-scale columns with a high catalyst volume fraction show a lower sensitivity to the reaction kinetic data.

Vapour permeation experiments with a binary 1-propanol/water mixture have been performed in a pilot-scale plant with a membrane area of 0.5 m<sup>2</sup> using the polymeric membrane Pervap<sup>TM</sup> 2201(D) from Sulzer Chemtech. The experiments proved the suitability of the membrane used and its stability at the operating conditions. In the measured concentration range, the membrane shows a high selectivity and high fluxes. In comparison to test cells with a smaller membrane area, a significant dewatering occurs in the pilot-scale module, changing the permeate fluxes along the membrane. The experimental results have been used to determine the required model parameters for the calculation of the overall transmembrane flux. The reactive hybrid process has been investigated with the validated detailed models for both stand-alone unit-operations. Comprehensive simulation studies illustrate the influence of structural and operational parameters on the process performance in terms of product purity and acid conversion.

The analysis of the variation of the reflux purity, which is a decisive variable for the performance of the hybrid process, shows contrary effects of the reboiler heat duty and the required membrane area. To solve the resulting optimisation problem, an evolutionary optimisation algorithm will be used in further activities.

## Acknowledgement

The authors wish to acknowledge the financial support provided by the European commission within the 6th Framework Programme, Project "INSERT-Integrating Separation and Reaction Technologies", Contract-No: NMP2-CT-2003-505862 and within the 5th Framework Programme, Marie Curie Training Site "Reactive Separations", Contract Nr. HPMT-CT-2001-00408. The support of "Fonds der Chemischen Industrie" with the required chemicals is highly appreciated.

## Nomenclature

$a_{ij}$	temperature-independent binary interaction parameter
$b_{ij}$	temperature-dependent binary interaction parameter (K)
$x_i$	molar fraction of component $i$ liquid phase (mol mol <sup>-1</sup> )
$a_i$	activity of component $i$ (mol mol <sup>-1</sup> )
$\gamma_i$	activity coefficient of component $i$
$\nu_i$	stoichiometric coefficient of component $i$
$c_{act}$	concentration of active sites (eq kg <sup>-1</sup> )
$m_{cat,dry}$	mass of dry catalyst (kg)
$k_f$	rate constant forward reaction (mol eq <sup>-1</sup> s <sup>-1</sup> )
$K_{eq}$	equilibrium constant
$R_m$	ideal gas constant

$n_c$	number of components
$T_{boil}$	temperature at boiling conditions (°C)
$T_{max, cat}$	maximum operating temperature of catalyst (°C)
$X_i$	conversion of component $i$
$D/F_{mass}$	distillate-to-feed ratio (kg kg <sup>-1</sup> )
$\psi_{cat}$	catalyst volume fraction (m <sup>3</sup> m <sup>-3</sup> )
$k_L$	liquid-phase mass-transfer coefficient (m s <sup>-1</sup> )
$k_G$	gas-phase mass-transfer coefficient (m s <sup>-1</sup> )
$h_L$	molar liquid hold-up (m <sup>3</sup> m <sup>-3</sup> )
$a_{eff}$	effective interfacial area (m <sup>2</sup> m <sup>-3</sup> )
$\Delta p$	pressure drop (bar)
$w_i$	mass fraction of component $i$ (kg kg <sup>-1</sup> )
$\Delta T_{sub}$	degree of superheating (°C)
$J$	total permeate flux (kg m <sup>-2</sup> h <sup>-1</sup> )
$J_i$	partial permeate flux of component $i$ (kg m <sup>-2</sup> h <sup>-1</sup> )
$\Delta DF$	transmembrane driving force
$p_i$	partial pressure of component $i$ (bar)
$v$	reflux ratio (mol mol <sup>-1</sup> )
$A_{memb}$	membrane area (m <sup>2</sup> )
$Q_H$	reboiler heat duty (W)

## References

- Hiwale, R. S., Mahajan, Y. S., Bhate, N. V., Mahajani, S. M., (2004) *Int. Journal of Chem. Reac. Eng.*, 2
- Kaibel, G., Miller, C., Holtmann, T., Schoenmakers, H., (2005) *Chem. Ing. Tech.*, 77, No.11, 1749-1758
- Rautenbach, R., *Membranverfahren- Grundlagen der Modul- und Anlagenauslegung*, Springer-Verlag, Berlin Heidelberg, 1<sup>st</sup> edn. (1997)
- Lipnitski, F. , Field, R. W., Ten, P., (1999) *J. Memb. Sci.*, 153, 183-210
- Kreis, P., Górak, A., (2006) *Chem. Eng. Res. Des.*, 84, 595-600
- Steinigeweg, S., Gmehling, J., (2004) *Chem. Eng. Proc.*, 43, 447-456
- von Scala, C., Fässler, P., Gerla, J., Maus, E., (2005) *Chem. Ing. Tech.*, 77, No. 11, 1809-1813
- Lundquist, E. G., (1995) *U.S. Patent 5 426 199*, Rohm and Haas Company
- Blagov, S., Parada, S., Bailer, O., Moritz, P., Lam, D., Weinand, R., Hasse, H., (2006) *Chem. Eng. Sci.*, 61, 753-765
- NIST Chemistry Web Book. <http://webbook.nist.gov/chemistry/>, December 2005

Tlatlik, S., (2005) *Internal report in the frame of the EU Project "INSERT-Integrating Separation and Reaction Technologies"*

Gmehling, J., *Azeotropic Data*, VCH Weinheim (1994)

Taylor, R., Krishna, R., (2000) *Chem. Eng. Sci.*, 55, 5183-5229

Noeres, C., Kenig, E. Y., Górak, A., (2003) *Chem. Eng. Proc.*, 42, 157-178

Kenig, E. Y., Górak, A. in Keil F. J. (ed.), *Modelling of Process Intensification*, Wiley-VCH, Weinheim, 1<sup>st</sup> edn. (2007)

Richter, J., Górak, A., Kenig, E. Y. in Schmidt-Traub, H. and Górak, A. (eds.), *Reactive distillation*, Springer, Heidelberg (2006)

Hayden, J. G., O'Connell, J. P., (1975) *Ind. Eng. Chem. Process Des. Dev.*, 14, No. 3, 209-216

Duarte, C., Buchaly, C., Kreis, P., Loureiro, J. M., (2006) *Inz. Chem. Procesowa*, 27, 273-286.

Klöker, M., Kenig, E. Y., Hoffmann, A., Kreis, P. Górak, A., (2005) *Chem. Eng. Proc.*, 44, 617-629

Górak, A., Hoffmann, A., (1999) *AIChE J.*, 47, No. 5, 1067-1076

Schneider, R., Noeres, C., Kreul, L. U., Górak, A., (1999) *Comp. Chem. Eng.*, 23, 423-426

Brunazzi, E., (2006) *Internal report in the frame of the EU Project "INSERT-Integrating Separation and Reaction Technologies"*

Brunazzi, E., Viva, A. in Sorensen, E. (ed.), *Distillation & Absorption 2006*, IChemE Symposium Series No. 152, ISBN 100852955057, 554-562, (2006)

Bravo, J. L., Rocha, J. A., Fair, J. R., (1985) *Hydrocarbon Processing*, 1, 91-95

Rocha, J. A., Bravo, J. L., Fair, J. R., (1993) *Ind. Eng. Chem. Res.*, 32, 641-651

DIN Deutsches Institut für Normung, Bestimmung der Totalen Kapazität von Kationenaustauscher, *DIN 54403*, Deutsche Norm (2000)

Buchaly, C., Kreis, P., Górak, A. in Sorensen, E. (ed.), *Distillation & Absorption 2006*, IChemE Symposium Series No. 152, ISBN 100852955057, 373-383, (2006)

Sulpak 3.0, Sulzer Chemtech Ltd., (2001)



Schmitt, M., *Heterogen katalysierte Reaktivrektifikation: Stoffdaten, Experimente, Simulation und Scale-up am Beispiel der Synthese von Hexylacetat*, PhD-Thesis, Institut für Technische Thermodynamik und Thermische Verfahrenstechnik, Universität Stuttgart, (2005)

van Baelen, D., Reyniers, A., van der Bruggen, B., Vandecasteele, C., Degreve, J., (2004) *Sep.Sci Tec.*, 39, 563-580

Stange, O. J., *Stofftransport durch eine hydrophile Polymermembran am Beispiel der Dampfpermeation*, PhD-Thesis, GKSS-Forschungszentrum Geesthacht GmbH, GKSS 2001/37 (2001)

Kreis, P., Górak, A. (2005) *Chem. Ing. Tech.*, 77, No. 11, 1737-1748